# Neck compartmentalization as the molecular basis for the different endocytic behaviour of Chs3 during budding or hyperpolarized growth in yeast cells

Carlos Sacristan, Abigail Reyes and Cesar Roncero*.

Instituto de Biología Funcional y Genómica and Departamento de Microbiología y Genética. CSIC/Universidad de Salamanca. Salamanca, Spain

Running title: Endocytosis and chitin synthesis regulation.

Key words: Chitin, Chs3, Chs4, endocytic turnover, septins, polarized growth.

*Corresponding author:

Cesar Roncero

Departamento de Microbiología y Genética. CSIC/Universidad de Salamanca.

Edificio Departamental. R-219

Avda. Campo Charro s/n.

37007-Salamanca

SPAIN

E-mail: crm@usal.es

Phone: 34-923-294733 FAX: 34-923-224876

## ABSTRACT

Yeast cells normally grow by budding, but under certain specific conditions they are also able to grow in hyperpolarized forms reminiscent of hyphal growth. During vegetative growth, the synthesis of the septum that physically separates yeast cells during cytokinesis depends on the correct assembly of the septin ring. Septins and actin patches are assembled at the neck, forming two concentric rings where the actin patch ring occupies the external-most part. This specific positioning defines a plasma membrane region at the neck from which other lateral membrane compartments are excluded. In this scenario, correct assembly of the chitin ring is dependent on the anchoring of Chs3 to the septin ring through Chs4. The anchoring of Chs3 to septins through Chs4 prevents the arrival of this protein at endocytic sites, thus reducing the endocytosis of Chs3. This allows an equilibrium to be set up between the antero- and retrograde transport of Chs3, facilitating the synthesis of the chitin ring at the neck. In contrast, hyperpolarized growth is characterized by a reduced endocytic turnover of Chs3, which in turn lead to the accumulation of Chs3 at the plasma membrane and a concomitant increase in chitin synthesis.

## INTRODUCTION

Yeast cells can switch between different forms of growth, including budding, mating and sporulation. In all these cases, cell integrity is maintained by the cell wall, an essential cellular structure that surrounds the yeast cell (Levin, 2005). A key element in yeast cell walls is chitin, which acts as scaffold for the assembly of the rest of the components of the structure (Kollar *et al.*, 1997). In yeast, but also in some other fungi (Banks *et al.*, 2005; Munro and Gow, 2001), most cellular chitin is synthesized by Chitin Synthase III, whose catalytic subunit is Chs3. CSIII activity depends on the arrival of Chs3 at the PM, a process that is facilitated by other accessory Chs proteins (Roncero, 2002). In *S. cerevisiae*, chitin synthesis differs significantly among the different forms of growth, which suggests specific mechanisms for the regulation of this activity (Roncero, 2002). This has been demonstrated during sporulation, in which the function of Chs4 during vegetative growth is replaced by Shc1, a homologue of Chs4 that is specifically induced during sporulation and that has partially redundant functions (Sanz *et al.*, 2002). Many years ago it was observed that chitin synthesis increases during mating, the polymer locating to the base of shmoos (Schekman and Brawley, 1979). More recently, it has been shown that chitin synthesis during mating depends on Chs4, Chs5 and Chs7, similar to what occurs during vegetative growth (reviewed in (Roncero, 2002), although very little is known about CSIII regulation during this process.

The synthesis of chitin during budding is a relatively well known process. Most chitin is assembled in a chitin ring at the mother side of the neck. This ring, although fully dispensable for cytokinesis, becomes essential when this process is minimally altered under a variety of conditions (Gomez *et al.*, 2009; Roncero and Sanchez, 2010). Its synthesis depends on the activation of CSIII at the PM but also on the anchoring of this activity to the neck, both processes being directly linked to the function of Chs4 (Reyes *et al.*, 2007; Sanz *et al.*, 2004; Trilla *et al.*, 1997). Chs4 is required for CSIII activation through an unknown mechanism, but Chs4 also interacts with Bni4, and this with the septin ring (DeMarini *et al.*, 1997; Kozubowski *et al.*, 2003), allowing correct assembly of the chitin ring (Sanz *et al.*, 2004). Chs3 is transported to the PM by the low-density pool of transport vesicles together with many other proteins (Sanchatjate and Schekman, 2006) and is later endocytosed (Holthuis *et al.*, 1998). However, contrary to most proteins Chs3 is not delivered to the vacuole but instead is recycled to

the TGN, from where it will eventually be delivered again to the PM (Valdivia *et al.*, 2002). A proper endocytic turnover of Chs3 is critical for the regulation of chitin synthesis, at least during vegetative growth. It has recently been shown that this turnover depends not only on the endocytic machinery but also on Chs4 function (Reyes *et al.*, 2007), although it is not known whether the role of Chs4 depends on its activating and/or anchoring functions.

The close relationship between endocytic recycling and protein polarization in yeast was established many years ago using the yeast mating process as a model (Valdez-Taubas and Pelham, 2003). However, further work indicated that not all proteins behaved in the same way (Proszynski *et al.*, 2006), which was explained in terms of alternative mechanisms in the maintenance of protein polarity during mating. In addition, there is no clear evidence indicating whether the same mechanisms are used during budding growth. Two recent reports, using completely different approaches, have addressed the mechanisms involved in the maintenance of Cdc42 polarity during the cell cycle. Apparently, endocytosis-mediated polarization can only be applied mechanistically to proteins with slow diffusion rates at the PM, thus excluding Cdc42 owing to its very rapid diffusion rate (Layton *et al.*, 2011). This model, initially theoretical, has recently been partially confirmed experimentally (Orlando *et al.*, 2011). However, there are still many unanswered questions in the field, since most of the proteins studied as models are directly or indirectly involved in the polarization process itself. In addition, no extensive studies have been carried out to compare the behaviour of PM proteins during vegetative growth or mating. A unique case in such studies is Wsc1, which is an integral PM protein that acts as a cell wall stress sensor and is therefore not involved in polarization itself (Levin, 2005). It localizes to the site of growth and its polarization has been shown to be fully dependent on endocytosis (Piao *et al.*, 2007). However, the localization of Wsc1 during mating has not been addressed.

Within this scenario Chs3 seemed to offer an alternative tool to study the relationship between polarization and endocytosis in yeast. Chs3 is an integral PM protein that behaves as a typical cargo protein delivered to the PM in a polarized fashion (Reyes *et al.*, 2007) and that is expressed both during vegetative growth and mating (Cos *et al.*, 1998); this allows comparisons to be made between both types of growth. In addition, Chs3 is mostly retained at the neck, providing a different view of how endocytosis might regulate protein trafficking around the neck region.

In the present work we describe the behaviour of Chs3 at the PM during budding and the different forms of hyperpolarized growth. We show that while the endocytic turnover of Chs3 is critical for protein localization during budding, the polarization of Chs3 during mating becomes mostly independent of its endocytic turnover. The analysis of Chs4 function during mating and budding explains the specific role of this protein in the regulation of Chs3 endocytosis at the neck, providing the basis for a mechanistic model that could explain the endocytic behaviour of other proteins.

## RESULTS

### *Cellular hyperpolarization apparently alters the intracellular behaviour of Chs3.*

We have previously demonstrated that proper synthesis of the chitin ring during vegetative growth depends on the correct endocytic turnover of Chs3, which is dependent at least on Chs4 function and on the endocytic machinery associated with actin patches (Reyes *et al.*, 2007). In addition, it has been known for many years that conjugation increases chitin synthesis, accompanied by an accumulation of the polymer at the base of shmoos (Schekman and Brawley, 1979). In light of these lines of evidence, we were interested in testing whether an alteration of the endocytic turnover of Chs3 during mating might be linked to the described effect on chitin synthesis and, if this indeed occurs, what the molecular reasons for the differences between vegetative growth and mating are.

First, we determined whether our hypothesis might be correct by comparing Chs3 localization during vegetative growth and mating. During the former (Figure 1A, upper row), a direct correlation was seen between the localization of septin Cdc3, Chs4, Chs3 and the chitin ring, as has been documented in independent works. During mating, mimicked experimentally throughout our work by α-factor treatment, chitin apparently colocalized with septin Cdc3, which acquired a characteristic barred distribution (Figure 1A lower row, (Versele and Thorner, 2005). However, Chs3 as well as Chs4 were distributed uniformly along the mating projection, even in zones where chitin synthesis was not apparent (Figure 1A, lower row). In addition, the localization of Chs3 in intracellular structures was not apparent and neither Chs3 nor Chs4 seemed to colocalize with septins. These results constitute preliminary but promising evidence about differences in the regulation of Chs3 during mating.

In order to determine whether these differences were related to the endocytic turnover of Chs3 or not, as an initial approach we next determined the apparent sites of endocytosis by analyzing the early stages of FM4-64 internalization (Zonia and Munnik, 2008). During vegetative growth, the FM4-64 signal labelled vesicles in the vicinity of the PM but, also, the fluorescence appeared concentrated at the neck region (Figure 1B). During polarized growth, the FM4-64 signal concentrated at the tip of the projection, revealing an apparently narrow region of endocytosis. This distribution was fairly similar to that of actin patches in both forms of growth (Figure 1C), in agreement with current models of endocytosis (Robertson *et al.*, 2009). Interestingly, the actin patches and endocytic sites colocalized with Chs3 during vegetative growth but not during mating (compare images in Figures 1B and C with those in Figure 1A).

These results suggested that the physical relationship between Chs3 and the endocytic machinery could be different during mating, promoting a different endocytic turnover of Chs3 that could be associated with its broader distribution.

***Positioning at the neck: A physical link between the anchoring of Chs3 at the neck and endocytosis.***

If our hypothesis were correct, the organization of the neck machinery during vegetative growth could be critical for the proper regulation of Chs3 and we therefore determined the specific positioning of Chs3, septin Cdc3 and actin patches with respect to other laterally distributed PM membrane proteins. We used two markers for different lateral membrane compartments: the $H^+$-ATPase Pma1, which defines the MCP (Membrane Compartment Occupied by Pma1), and Sur7, a component of the MCC (Membrane Compartment Occupied by Can1), which is distributed in discrete patched structures, also called eisosomes (Grossmann *et al.*, 2007). Both compartments are non-overlapping (Lauwers *et al.*, 2007) and are excluded from the neck and the early emerging bud (Moreira *et al.*, 2009). Reconstructed frontal images revealed the presence of a clear Chs3-GFP ring at the neck that was optically separated from the Pma1-mCherry and Sur7-mRFP signals. In addition, the images showed an empty ring between Chs3 and both PM proteins (Figure 2A). Similar results were obtained in middle sections, where –consistently- a gap between the green and red signals was observed (Figure 2B, see also Figure S1 in Supplementary Materials). Septins act as the physical link of Chs3 to the neck (DeMarini *et al.*, 1997), but they also act as a barrier

to physical diffusion (Caudron and Barral, 2009). Accordingly, we colocalized Cdc3-GFP with Pma1 and Sur7. Surprisingly, the exclusion zone between Cdc3-GFP and the PM markers was also clearly visible in frontal (Figure 2A) and sectional (Figure 2B, see also Figures S1 and S2 at supplementary materials) images. We later stained actin with Alexa fluor 488-conjugated phalloidin to position the actin patch ring with respect to Pma1 and Sur7. In this case, we did not observe an exclusion zone, the ring of actin patches appearing in physical contact with both PM proteins, as seen in frontal and middle sections (Figure 2 A, B). Very similar results were obtained for Gap1 (not shown) and hence it may be assumed that the exclusion region observed around the neck affects all laterally distributed transmembrane proteins.

From this evidence it may be deduced that it is the ring of actin patches that delimits the exclusion zone between Chs3/septins and lateral membrane proteins. If this hypothesis were correct, then the exclusion zone would be dependent on actin. The depolymerization of actin after latA treatment redistributed Chs3 along the PM (Figure 2C), as described previously (Reyes *et al.*, 2007). More importantly, however, Pma1 diffused into the neck region, abolishing the previously described exclusion zone (Figure 2C, see also Figure S2B at supplementary materials). Very similar results were obtained using the more stable neck marker Cdc3-GFP (Figure 2C, see also Figure S2A in supplementary materials). In addition, depletion of $PIP_2$ by overexpression of the human PIP3 kinase (Rodríguez-Escudero *et al.*, 2005) delocalized actin patches producing a redistribution of Chs3 from the neck and abolished PM compartmentalization around the septin ring (Figure 2D, see also Figure S2A). However, it could be argued that any of these treatments have pleiotropic effects and hence we tested the effect of Syp1 deletion. Syp1 interacts with septins (Qiu *et al.*, 2008), forming a distinct ring around the neck that allows the polarization of actin patches within the neck region (Figure 2E). In the *syp1*Δ mutant, actin patches delocalized without significantly affecting the rate of endocytosis (Stimpson *et al.*, 2009), but Chs3 became partially redistributed from the neck along the PM and the exclusion zone from Pma1 disappeared (Figure 2F, see also Figure S2B). Apparently, the exclusion zone observed at the neck depends not only on the assembly of the actin patches, but also on their localization at the neck region.

The images described above also suggested the organization of the proteins in rings of different diameters, and this was indeed the case. While the diameters of the

Cdc3-GFP and Chs3-GFP rings were virtually identical, the diameter of the actin patch rings was significantly larger than those of Chs3 or Cdc3 (Figure 3A). Moreover, the rings of actin patches always appeared outside those of Chs3 and had a larger diameter, as shown in the line-scan (Figure 3B). Mid-sectional images (Figure 3C) indicated that the actin patches were typically displaced to the mother side of the neck with respect to the Chs3 ring, which only became flanked at both sides very late during the cell cycle (Figure 3B, lower image). Unfortunately, it became technically impossible to determine the diameter of the exclusion zone in a statistically representative number of cells.

The combination of optical and numerical data can provide a reliable model for the assembly of the different neck components (Figure 3D). Based on previous evidence, septins would establish the physical localization of Chs3 through Chs4 and Bni4. Very likely most Chs3 would accumulate at the mother side because of the physical barrier to diffusion formed by the septins at the PM (Caudron and Barral, 2009). The actin patches would form a wider and more external ring on the mother cell, defining a second diffusion barrier that physically separates the neck compartment from the rest of the lateral plasma membrane proteins. Interestingly, the Chs3 ring appeared to be flanked by actin patches on both sides of the neck in cells finishing their process of cytokinesis (Figure 3C, lower panel), clearly confirming the physical exclusion between the Chs3 and the actin patch ring.

It is expected that this organization would be responsible for the regulation of Chs3 endocytic turnover in a wt cell (see Discussion for further arguments) and hence this turnover would be altered in the absence of Chs3 anchorage to the neck, as in the *chs4*Δ mutant (Reyes *et al.*, 2007), or after the depolymerization (Figure 2C) or delocalization (Figure 2F) of actin.

***Hyperpolarized growth alters the endocytic turnover of Chs3.***

The next step focused on what occurs during mating, which would be necessarily different since *S.cerevisiae* cells grow in a hyperpolarized form without the presence of an apparent neck. During this form of growth, chitin synthesis increased 3-4-fold and chitin accumulated at the base of shmoos in a localization roughly similar to that of the septins (Figure 1A). Chs3-GFP and Chs4-GFP were uniformly distributed along the mating projection, even at the tip regions devoid of chitin and septins (Figure 1A), in sharp contrast with the perfect co-localization of chitin, septins, and Chs3/Chs4 during vegetative growth (Figure 1A). The first issue was to address how these proteins

are delivered to the mating projection by using controlled expression from the *GAL1* promoter. Chs3 was visible at the tip of the mating projections approximately 60 minutes after induction and its distribution area increased steadily up to 120 minutes after induction, when it reached a maximum that was not affected by longer induction times (Figure 4). The distribution area achieved was similar to that observed in mating cells grown overnight in galactose (see Fig S3 for additional information). Chs4 seemed to be delivered in a similar way, since it was visible at the tip only 30 minutes after induction. Later, it became distributed along the projection (Figure 4). However, longer induction times produced a fairly uniform distribution throughout the cell membrane (Figure 4, see also Figure S3). Together, these results indicated that Chs3 and Chs4 were delivered to the tip of the mating projection, later becoming redistributed along the PM of the projection. However, at the base of the shmoos there seemed to be a physical barrier that was much more effective at blocking Chs3 than Chs4 diffusion to the body cell.

We have previously shown that Chs3 localization depends strictly on Chs4 and endocytic recycling during vegetative growth (Reyes *et al.*, 2007). Accordingly, we next addressed the role of both in the localization of Chs3 during mating. Chs4 is required for chitin synthesis during mating (Trilla *et al.*, 1997), but to our surprise Chs3 localization was apparently independent of Chs4 (Figure 5A) and the protein accumulated at the PM in its absence, contrary to what occurs during budding (Reyes *et al.*, 2007). Very similar results were obtained during the hyperpolarized growth induced by the depletion of the mitotic cyclin dependent kinase Cdc28, where Chs3 was also distributed along the PM of the polarized projection, and its distribution was not affected by the absence of Chs4 (see supplementary materials Figure S4). Thus, Chs3 localization at the PM during hyperpolarized growth did not require Chs4, suggesting that Chs3 polarization would be independent of endocytosis. To test this hypothesis, we compared the behaviour of Chs3 with that of Snc1, a transmembrane protein whose polarization has been shown to depend on endocytosis during both budding and mating (Proszynski *et al.*, 2006; Valdez-Taubas and Pelham, 2003). We first addressed Chs3 localization in the *end4*Δ mutant. Chs3 remained localized along the cell despite the formation of shmoos (Figure 5B), similarly to what has been described for Snc1 (Proszynski *et al.*, 2006). Very similar results were obtained when α-factor was added to cells pre-treated with latA (not shown). We next tested the effect of latA addition during the budding and mating processes. During vegetative growth, latA treatment

abolished Chs3 and Snc1 polarization at only 35 minutes after its addition (Figure 5C). In contrast, when latA was added at 25 (Figure 5D) or 120 minutes (Figure 5E) after α-factor, the polarization of Chs3 remained stable after the same 35 minutes, but Snc1 polarization was severely altered since the protein was distributed along the cell. We also tested Chs3 localization in the yeast amphiphysin *rvs161*Δ mutant, which showed reduced rates of endocytosis (Munn *et al.*, 1995). Chs3 polarization was maintained during mating in the *rvs161*Δ, but also in the *syp1*Δ mutant or after PI3K overexpression (Figure S5). Apparently, endocytosis is not required for the maintenance of Chs3 polarization during mating, as occurs for Snc1, but is required for triggering the polarization of both Chs3 and Snc1 at the beginning of hyperpolarized growth. Together, all this evidence suggests that the endocytic recycling of Chs3 is reduced during mating as compared to vegetative growth, explaining its higher accumulation at the PM (not shown) and also its absence in intracellular structures (Figures 1 and 5).

At this point, we wondered whether this idea was also valid for other forms of hyperpolarized growth such as the switch between the yeast and mycelial growth patterns seen in *C. albicans*. To address this question, we tagged a chromosomal copy of CaChs3 with the appropriate version of the GFP (see Materials and Methods). CaChs3-GFP localized to the neck and intracellular vesicles during yeast growth (Figure 6A, leftmost panel), as previously described (Lenardon *et al.*, 2010). The induction of filamentous growth with FBS led to an immediate redistribution of Chs3 along the PM and, shortly after that, to the polarization of Chs3 towards the tip of the filamentous tube (Figure 6A). The polarization of Chs3 persisted during the filamentation process and the accumulation of Chs3 at intracellular compartments became evident after filamentation had proceeded further (Figure 6A, right panels). The addition of latA during filamentation produced hyphal tip swelling, although CaChs3 remained polarized after 40 minutes (Figure 6B). Surprisingly, CaChs3 polarization still occurred when filamentation was induced in the presence of latA (Figure 6C), although the formation of hyphae was almost completely abolished (not shown).

In conclusion, it seems that Chs3 polarization during hyperpolarized growth does not depend on its endocytic turnover, contrary what occurs during budding, suggesting a rapid and efficient mechanism for increasing the amount of CSIII at the PM and the concomitant increase in chitin synthesis reported during mating in *S.cerevisiae* and during hypha formation in *C.albicans*.

## DISCUSSION

### *Chs3 as an alternative model to study cell polarity in yeast.*

For many years *S. cerevisiae* has been a very useful tool for the study of cell polarity because its molecular genetics readily allows the possibility of unravelling the unknown aspects of this process. However, there are still many conflictive points in our understanding of how this process is regulated, and currently there is still some controversy about the specific role of endocytic turnover in the maintenance of polarity of some proteins.

Along this paper we have shown that Chs3 is an alternative model for the study of cell polarity in yeast. Chs3 is an integral PM protein whose delivery is highly polarized, both during vegetative growth (Reyes *et al.*, 2007) and during mating (Figure 4 and 5, this work). This polarization also seems to persist during alternative forms of hyperpolarization (Figure 6, Figure S4). Interestingly, our results indicate that the polarization of Chs3 at the PM follows different rules during vegetative and hyperpolarized growth. While during budding the exquisite equilibrium between anterograde and retrograde transport is required for Chs3 polarization and its correct localization, during mating the anterograde transport of Chs3 is dominant, producing a polarized accumulation of Chs3 in the membrane. These differences make Chs3 localization fully dependent on Chs4 and endocytosis during budding, while it is independent of them during hyperpolarized growth.

### *Neck compartmentalization as a tool for regulating the endocytic turnover of Chs3.*

During budding the physical distribution of different proteins at the neck would explain the specific role of the anchoring of Chs3 to the neck. The neck proteins studied here were distributed in fairly concentric rings, with the Chs3 and septin rings physically co-localizing, in clear agreement with previous observations (DeMarini *et al.*, 1997; Kozubowski *et al.*, 2003; Sanz *et al.*, 2004). Actin patches would form an external and wider ring. Our results suggest that the patches of actin constitute the physical limit for the lateral distribution of PM proteins such as Pma1 or Sur7, but also of Chs3, since the elimination of actin patches by latA or simply their depolarization in the absence of Syp1 (Stimpson *et al.*, 2009) abolished the exclusion zone for Pma1 around the neck, also promoting a redistribution of Chs3. But how does the actin ring

delimit the neck compartment? One hypothesis would be that the ring of actin patches assembled around the septins would act as a drainage ring, preventing the lateral diffusion of PM proteins and facilitating their endocytic recycling. In addition, it is likely that the positioning of actin patches would affect directly membrane composition, contributing to the generation of a physical barrier. In agreement with this proposal, the depletion of $PIP_2$ at the PM also abolished the compartmentalization of the neck membrane (Figure 2D), in accordance with the proposed role for these lipids in membrane compartmentalization and their specific accumulation at the neck (Garrenton *et al.*, 2010).

How does Chs3 turnover regulation fit into this neck-membrane compartmentalized model? Chs3 is delivered to the neck by polarized transport, and in the presence of Chs4 it becomes properly anchored and would become physically separated from the endocytic region defined by the actin patch ring. Only the Chs3 molecules released from the septin ring would diffuse freely through the neck compartment, becoming endocytosed. This release was visualized in some cells as a gradient of Chs3-GFP from the neck (Figure 2A, insert) and would probably be promoted by the incorporation of new molecules of Chs3 delivered by anterograde transport. Under normal circumstances, an equilibrium would exist between antero- and retrograde transport that would lead to the proper regulation of chitin synthesis. This equilibrium would probably be different between mother and bud cells and could explain the partially different behaviour of Chs3 in the late stages of the cell cycle (Zanolari *et al.*, 2011). In the absence of Chs4, Chs3 would not anchor to the neck and would therefore diffuse towards the actin patch ring and immediately become endocytosed. In this case, retrograde transport would be favoured, leading to an accumulation of Chs3 in intracellular vesicles (Reyes *et al.*, 2007). This is also likely to occur during the part of the cell cycle when Bni4 and Chs4 are not localized to the neck and Chs3 is only visible in intracellular structures (Kozubowski *et al.*, 2003).

***An escape from endocytosis:the behaviour of Chs3 during hyperpolarized growth.***

Our results also clearly support the different behaviour of Chs3 during hyperpolarized growth. This behaviour can be envisaged as being similar to that reported after latA treatment (Reyes *et al.*, 2007) or PKC activation (Valdivia and Schekman, 2003) during vegetative growth, in which the anterograde transport of Chs3

is predominant, allowing the accumulation of Chs3 at the PM and a significant increase in chitin synthesis. Many explanations could be invoked to account for alterations in the equilibrium between the antero- and retrograde transport, but it is unlikely that a simple increase in Chs3 expression would be responsible for this effect, because although such as increase is known to occur during mating (Cos *et al.*, 1998) it does not occur in the case of the *cdc28*$^{ts}$ mutant (Figure S4) or during hypha formation in *C.albicans* (Kadosh and Johnson, 2005). Our results instead point to a reduced endocytosis of Chs3 during hyperpolarized growth, because Chs3 localization became independent of Chs4 (a known regulator of the endocytic recycling of Chs3 during budding), and was not affected in the *rvs161*Δ and *syp1*Δ endocytic mutants. In addition, it was unaffected by the endocytic blockade produced by latA treatment. This latter observation is in clear contrast to what occurs for Snc1, whose polarization depends directly on endocytic recycling (Figure 5D, E and (Valdez-Taubas and Pelham, 2003). Since both Snc1 and Chs3 depend on endocytosis for localization during budding, it seems clear that a reduced endocytic turnover of Chs3 during mating could explain the differences observed. However, we cannot exclude a specific increase in the anterograde transport of Chs3 during mating, which could partially contribute to its accumulation at the PM. This model seems valid for most, if not all, forms of hypolarized growth, since it is fully compatible with our results regarding cdc28$^{ts}$ mutants and the induction of filamentation in *C.albicans*. A seemingly contradictory result in this scheme is the absence of polarization of Chs3 (Figure 5B) and Snc1 (Proszynski *et al.*, 2006) during mating in the *end4*Δ mutant. However, the biological functions of both proteins depend on an endocytic pool (Lewis *et al.*, 2000) that is depleted in *end4*Δ cells, and hence the *de novo* synthesis of these proteins does not seem sufficient for a polarized distribution to be achieved. However, CaChs3 remains polarized during filamentation in the presence of latA. The most plausible explanation is that incorporation of CaChs3 to the PM would depend to a greater extent on *de novo* synthesis than in *S.cerevisiae*.

The different behaviour of Chs3 and Snc1 during mating can be explained simply in terms of their different biological roles. Snc1 is an integral part of the machinery involved in polarized secretion and hence its localization should be maintained very precisely (Figure 5E and (Proszynski *et al.*, 2006)) by its continuous recycling. However, Chs3 behaves strictly as a cargo and can therefore diffuse freely along the PM, diminishing its endocytosis. Although direct measurement of the

diffusion rate of Chs3 at the PM has not been achieved, its rapid endocytosis in the absence of neck anchoring during budding suggests a rapid diffusion of the protein to access endocytic sites. Such a diffusion rate would discriminate Chs3 from other slow-diffusion rate proteins such as Snc1 (Valdez-Taubas and Pelham, 2003), thereby explaining the differences observed. These differences were not apparent during budding due to the anchoring of Chs3 to the septin ring, which delays its lateral diffusion (see above).

In conclusion, on the basis of our chitin synthase model we show that the different accessibility to the endocytic machinery during hyperpolarized or vegetative growth could be sufficient for the differential regulation of the endocytic turnover of a given protein. This provides not only a way to change the behaviour of a protein between budding or hyperpolarized growth but also to discriminate the behaviour of different proteins. In addition it could be envisaged as a general mechanism to modify protein accumulation at the PM during specific stages the yeast cell life cycle.

## MATERIALS AND METHODS

### Yeast Strains and plasmids.

Most yeast strains used here were based on two different genetic backgrounds: W303 for vegetative growth and 15Daub (*bar1*Δ) for mating experiments. When required, gene deletions were made in the original strains using the gene replacement technique with different deletion cassettes based on auxotrophic markers (Reyes *et al.*, 2007) or *natMX4* resistance. *natMX4* resistance cassettes were used for *CHS3, CHS4* and *SYP1* deletions and were generated by PCR using pAG25 as template (Goldstein and McCusker, 1999). Similarly, Pma1 and Syp1 were tagged chromosomally at their C-terminus with mCherry, using an integrative cassette amplified from a pFA6-*natMX4* derivative (Hentges *et al.*, 2005). Sur7-mRFP strains were made by integrating the linearized YIp211-SUR7mRFP, as described (Grossmann *et al.*, 2007).

The *C. albicans* CAI4-*CaCHS3-GFP* strain was constructed as follows. *CaCHS3* was tagged chromosomally at its C-terminus with *eGFP3* using an integrative cassette constructed in several steps. First, the last 523 bp of the *CaCHS3* ORF were amplified with the CaCHS3-N1 (GTTACCAGCAGCCATTAC) and CaCHS3-

N2(SmaI) (GCTTTAACCCAATCACCCGGGACTGGACCCTGAAGAAG) primers, and cloned into the pGEM-T (pGEM-T::CaCHS3Nt) plasmid. Then, the 3' region of CaCHS3 comprising the 839 bp from the stop codon was amplified with primers CaCHS3-C1(SmaI) (CTTCTTCAGGGTCCAGTCCCGGGTGATTGGGTTAAAGC) and CaCHs3-C2 (GAGGTTTGACGTCAGTTG) and cloned into the pGEM-T (pGEM-T–CaCHS3Ct) plasmid. Following this, the *CaCHS3Ct* fragment was excised with XmaI/NcoI and subcloned into plasmid pGEM-T::CaCHS3Nt linearized with the same enzymes. In the resulting plasmid, which contained the reconstructed C-terminal region of *CaCHS3,* we introduced the *eGFP3* tag (Cormack *et al.*, 1997) as a SmaI/StuI fragment at the regenerated SmaI site immediately before the stop codon. Finally, *CaURA3* was subcloned as a NotI/XbaI fragment into a native SnaBI restriction site situated 251 bp downstream from the stop codon, affording the CRM964 plasmid. The integration cassette of about 3500 bp was excised from this plasmid with SacI/SphI and transformed into the CAI4 strain with the lithium acetate method. Transformants were selected on YNB w/o amino acids and confirmed by PCR with external oligonucleotides.

The *CHS3* and *CHS4* genes were always expressed from the centromeric plasmids pRS314 or pRS315 and protein localization was always assayed in their corresponding gene-deleted strains. In contrast, Cdc3-GFP and Syp1-GFP were always observed in wt strains. Most of the plasmids used have been described previously.

For a complete list of the yeast strains and plasmids used through this work see supplementary materials Table S1.

**Media and growth conditions.**

*S. cerevisisae* was grown in YEPD (1% yeast extract, 2% peptone, and 2% glucose) or synthetic minimal medium (SC) (2% glucose and 0. 7% yeast nitrogen base without amino acids) supplemented with the appropriate amino acids to maintain plasmid selection. Cells were incubated at 28ºC, except for the *cdc28-13* mutant, which was typically grown at the permissive temperature of 25ºC before shifting it to the restrictive temperature of 32ºC. For galactose induction, the yeast strains were grown in 2% raffinose media to early logarithmic phase and induction was triggered by adding galactose at a final concentration of 2%. Proteins were visualized at different times after induction.

Mating was mimicked experimentally by α-factor treatment in the 15Daub strains. Shmoo formation was usually assayed by adding α-factor at 200ng/ml for two hours, although shorter times of treatment were also used, as indicated. Endocytosis was blocked with latrunculin A at a final concentration of 15 µM (Reyes *et al.*, 2007). Microscopic observations were begun 15 minutes after treatment. The effects of PI3K overexpression (Rodriguez-Escudero et al., 2005) were typically determined 30 minutes after the addition of galactose.

*C. albicans* cells were grown as yeasts in YEPD at 28ºC. Hypha formation was induced by supplementing the growing media with 20% foetal bovine serum and further incubation at 37°C. Endocytosis in *C. albicans* was blocked using 50µM LatA.

**Microscopy**

Calcofluor vital staining was observed in cells grown in the presence of 50 µg/ml calcofluor for 2 hours at 28ºC (Gomez *et al.*, 2009). Transformant cells expressing GFP, and the mCherry or mRFP fusions were grown in SD medium supplemented with 0.2% adenine and visualized directly by fluorescence microscopy in living cells. Cdc11 was immunolocalized as described (Sanz *et al.*, 2004), using an anti-cdc11 (Santa Cruz Biotechnology, Santa Cruz, Ca. USA) as primary antibody and an anti-rabbit antibody coupled to Alexa fluor 488 as secondary antibody (Invitrogen Molecular Probes, Carlsband, Ca. USA).

For actin visualization, a 6-ml culture of cells was fixed with 2 ml of 16% formaldehyde (Polyscience, Warnington, USA) and 1 ml of PM Buffer (25 mM $K_2HPO_4$, pH 6.8, 0.5 mM $MgSO_4$) for one hour at 28ºC under conditions of constant shaking. Cells were pelleted at 1800xg for 5 min and washed three times with PM buffer. They were then permeabilized by resuspending them several times in 1 ml of PM buffer supplemented with 0.5% Triton X-100. The detergent was removed with repeated washes and the cells were finally resuspended in 50 µl of PM buffer. One µl of this cell suspension was incubated for one hour in the darkness with 5 µl of Alexa Fluor-488 or Alexa Fluor-568 phalloidin prepared previously according to the manufacturer's instructions (Invitrogen Molecular Probes).

To mark the sites of endocytosis, typically FM4-64 was added at a 10 mM concentration to the cell cultures. Immediately after the addition of FM4-64, cells were washed twice with cold SD medium and observed with fluorescence microscopy.

Most single-channel images were taken on a Leica RX150 (Leica Mycrosystems, Wetzlar, Germany) epifluorescence microscope with a 100 W Hg lamp, using the appropriate filters, as described (Reyes *et al.*, 2007). Two-channel images were acquired on a DeltaVision device (×100 objective; NA:1.40). Z-stack sections were collected at 0.20 μm steps and later deconvoluted using Softworx™ (Applied Precision, Issaquah, Washington, USA). Additionally, frontal sections of the rings were volume-reconstructed using the same software. The images were then processed using Image J and Adobe Photoshop CS3 (San José, Ca. USA) software. Linescans were performed in MetaMorph 7.1 (Molecular Devices, Sunnyvale, Ca. USA) and the data were transferred to Microsoft Excel for further analysis.

When required, image measurements were evaluated statistically using Student´s "t" test for unpaired data. Analyses were performed using the SPSS Statics 17.0 (IBM, New York, USA) software. Significantly different values ($p < 0.05$) are indicated (#).



## ACKNOWLEDGMENTS

We thank M.I Geli and J.Encinar for critical comments about the manuscript and for many years of fruitful discussions. Special thanks are due to W.Tanner, P.O. Ljungdahl, J.L. Revuelta, A.Spang, V.Cid and C.R. Vazquez for providing us with strains, plasmids and reagents; to R.Valle and V. Casquero for technical assistance, and to N. Skinner for language revision. C.S. was supported by a FPU fellowship from the MEC. This research was supported by the Spanish CICYT grants BIO2007-60779 and BFU2010-18632. Partial support from the JCyL through grants SA127A08 and GR231 is also acknowledged.

## REFERENCES

Banks, I.R., Specht, C.A., Donlin, M.J., Gerik, K.J., Levitz, S.M., and Lodge, J.K. (2005) A chitin synthase and its regulator protein are critical for chitosan production and growth of the fungal pathogen Cryptococcus neoformans. *Eukaryot Cell* **4**: 1902-1912.

Caudron, F., and Barral, Y. (2009) Septins and the lateral compartmentalization of eukaryotic membranes. *Dev Cell* **16**: 493-506.

Cormack, B.P., Bertram, G., Egerton, M., Gow, N.A., Falkow, S., and Brown, A.J. (1997) Yeast-enhanced green fluorescent protein (yEGFP)a reporter of gene expression in *Candida albicans*. *Microbiology* **143**: 303-311.

Cos, T., Ford, R.A., Trilla, J.A., Duran, A., Cabib, E., and Roncero, C. (1998) Molecular analysis of Chs3p participation in chitin synthase III activity. *Eur. J. Biochem.* **256**: 419-426.

DeMarini, D.J., Adams, A.E.M., Fares, H., De Virgilio, C., Valle, G., Chuang, J.S., and Pringle, J.R. (1997) A septin-based hierarchy of proteins required for localized deposition of chitin in the *Saccharomyces cerevisiae* cell wall. *J. Cell Biol.* **139**: 75-93.

Garrenton, L.S., Stefan, C.J., McMurray, M.A., Emr, S.D., and Thorner, J. (2010) Pheromone-induced anisotropy in yeast plasma membrane phosphatidylinositol-4,5-bisphosphate distribution is required for MAPK signaling. *Proc Natl Acad Sci USA* **107**: 11805-11810.

Goldstein, A.L., and McCusker, J.H. (1999) Three new dominant drug resistance cassettes for gene disruption in Saccharomyces cerevisiae. *Yeast* **15**: 1541-1553.

Gomez, A., Perez, J., Reyes, A., Duran, A., and Roncero, C. (2009) Slt2 and Rim101 contribute independently to the correct assembly of the chitin ring at the budding yeast neck in *Saccharomycces cerevisiae*. *Eukaryot. Cell* **8**: 1449-1559.

Grossmann, G., Opekarová, M., Malinsky, J., Weig-Meckl, I., and Tanner, W. (2007) Membrane potential governs lateral segregation of plasma membrane proteins and lipids in yeast. *EMBO J* **26**: 1-8.

Hentges, P., Van Driessche, B., Tafforeau, L., Vandenhaute, J., and Carr, A.M. (2005) Three novel antibiotic marker cassettes for gene disruption and marker switching in *Schizosaccharomyces pombe*. *Yeast* **22**: 1013-1019.

Holthuis, J.C., Nichols, B.J., and Pelham, H.R. (1998) The syntaxin Tlg1p mediates trafficking of chitin synthase III to polarized growth sites in yeast. *Mol. Cell. Biol* **9**: 3383-3397.

Kadosh , D., and Johnson, A.D. (2005) Induction of the *Candida albicans* filamentous growth program by relief of transcriptional repression: a genome-wide analysis. *Mol Biol Cell* **16**: 2903-2912.

Kollar, R., Reinhold, B.B., Petrakova, E., Yeh, H.J., Ashwell, G., Drgonova, J., Kapteyn, J.C., Klis, F.M., and Cabib, E. (1997) Architecture of the yeast cell wall. Beta(1-->6)-glucan interconnects mannoprotein, beta(1-->)3-glucan, and chitin. *J.Biol.Chem.* **272**: 17763-17775.

Kozubowski, L., Panek, H., Rosenthal, A., Bloecher, A., DeMarini, D.J., and Tatchell, K. (2003) A Bni4-Glc7 phospatase complex that recruit chitin synthase to the site of bud emergence. *Mol. Biol. Cell.* **14**: 26-39.

Lauwers, E., Grossmann, G., and André, B. (2007) Evidence for coupled biogenesis of yeast Gap1 permease and sphingolipids: essential role in transport activity and normal control by ubiquitination. *Mol Biol Cell* **18**: 3068-3080.

Layton, A.T., Savage, N.S., Howell, A.S., Carroll, S.Y., Drubin, D.G., and Lew, D.J. (2011) Modeling vesicle traffic reveals unexpected consequences for cdc42p-mediated polarity establishment. *Curr Biol* **21**: 184-194.

Lenardon, M.D., Milne, S.A., Mora-Montes, H.M., Kaffarnik, F.A., Peck, S.C., Brown, A.J., Munro, C.A., and Gow, N.A. (2010) Phosphorylation regulates polarisation of chitin synthesis in *Candida albicans*. *J. Cell Sci.* **123**: 621-629.

Levin, D.E. (2005) Cell wall integrity signaling in Saccharomyces cerevisiae. *Microbiol Mol Biol Rev.* **69**: 262-291.

Lewis, M.J., Nichols, B.J., Prescianotto-Baschong, C., Riezman, H., and Pelham, H.R. (2000) Specific retrieval of the exocytic SNARE Snc1p from early yeast endosomes. *Mol Biol Cell* **11**: 23-38.

Moreira, K.E., Walther, T.C., Aguilar, P.S., and Walter, P. (2009) Pil1 controls eisosome biogenesis. *Mol Biol Cell* **20**: 809-818.

Munn, A.L., Stevenson, B.J., Geli, M.I., and Riezman, H. (1995) *end5*, *end6*, and *end7*: mutations that cause actin delocalization and block the internalization step of endocytosis in *Saccharomyces cerevisiae*. *Mol Biol Cell* **6**: 1721-1742.

Munro, C.A., and Gow, N.A.R. (2001) Chitin synthesis in human pathogenic fungi. *Med Mycol* **39 (Suplement I)**: 41-53.

Orlando, K., Sun, X., Zhang, J., Lu, T., Yokomizo, L., Wang, P., and Guo, W. (2011) Exo-endocytic trafficking and the septin-based diffusion barrier are required for the maintenance of Cdc42p polarization during budding yeast asymmetric growth. *Mol Biol Cell* **22**: 624-633.

Piao, H.L., Machado, I.M., and Payne, G.S. (2007) NPFXD-mediated endocytosis is required for polarity and function of a yeast cell wall stress sensor. *Mol Biol Cell* **18**: 57-65.

Proszynski, T.J., Klemm, R., Bagnat, M., Gaus, K., and Simons, K. (2006) Plasma membrane polarization during mating in yeast cells. *J Cell Biol* **173**: 861-866.

Qiu, W., Neo, S.P., Yu, X., and Cai, M. (2008) A novel septin-associated protein, Syp1p, is required for normal cell cycle-dependent septin cytoskeleton dynamics in yeast. *Genetics* **180**: 1445-1457.

Reyes, A., Sanz, M., Duran, A., and Roncero, C. (2007) Chitin synthase III requires Chs4p-dependent translocation of Chs3p into the plasma membrane. *J. Cell Sci.* **120**: 1998-2009.

Robertson, A.S., Smythe, E., and Ayscough, K.R. (2009) Functions of actin in endocytosis. *Cell Mol Life Sci* **66**: 2049-2065.

Rodríguez-Escudero, I., Roelants, F.M., Thorner, J., Nombela, C., Molina, M., and Cid, V. (2005) Reconstitution of the mammalian PI3K/PTEN/Akt pathway in yeast. *Biochem J* **390**: 613-623.

Roncero, C. (2002) The genetic complexity of chitin synthesis in fungi. *Curr Genet.* **41**: 367-378.

Roncero, C., and Sanchez, Y. (2010) Cell separation and the maintenance of cell integrity during cytokinesis in yeast: the assembly of a septum. *Yeast* **27**: 521-530.

Sanchatjate, S., and Schekman, R. (2006) Chs5/6 complex: a multiprotein complex that interacts with and conveys chitin synthase III from the trans-Golgi network to the cell surface. *Mol. Biol. Cell* **17**: 4157-4166.

Sanz, M., Trilla, J.A., Duran, A., and Roncero, C. (2002) Control of chitin synthesis through Shc1p, a functional homologue of Chs4p specifically induced during sporulation. *Mol Microbiol.* **43**: 1183-1195.

Sanz, M., Castrejon, F., Duran, A., and Roncero, C. (2004) Saccharomyces cerevisiae Bni4p directs the formation of the chitin ring and also participates in the correct assembly of the septum structure. *Microbiology* **150**: 3229-3241.

Schekman, R., and Brawley, V. (1979) Localized deposition of chitin on the yeast cell surface in response to mating pheromone. *Proc. Natl. Acad. Sci. USA.* **76**: 645-649.

Stimpson, H.E., Toret, C.P., Cheng, A.T., Pauly, B.S., and Drubin, D.G. (2009) Early-arriving Syp1p and Ede1p function in endocytic site placement and formation in budding yeast. *Mol Biol Cell* **20**: 4640-4651.

Trilla, J.A., Cos, T., Duran, A., and Roncero, C. (1997) Characterisation of *CHS4* (*CAL2* ), a gene of *Saccharomyces cerevisiae* involved in chitin biosynthesis and allelic to *SKT5* and *CSD4*. *Yeast* **13**: 795-807.

Valdez-Taubas, J., and Pelham, H.R. (2003) Slow diffusion of proteins in the yeast plasma membrane allows polarity to be maintained by endocytic cycling. *Curr Biol* **13**: 1636-1640.

Valdivia, R.H., Baggot, D., Chuang, J.S., and Schekman, R. (2002) The yeast Clathrin adaptor protein complex 1 is required for the efficeint retention of a subset of late Golgi membrane proteins. *Dev. Cell* **2**: 283-294.

Valdivia, R.H., and Schekman, R. (2003) The yeasts Rho1p and Pkc1p regulate the transport of chitin synthase III (Chs3p) from internal stores to the plasma membrane. *Proc. Natl. Acad. Sci. U S A* **100**: 10287-10292.

Versele, M., and Thorner, J. (2005) Some assembly required: yeast septins provide the instruction manual. *Trends Cell Biol* **15**: 414-424.

Zanolari, B., Rockenbauch, U., Trautwein, M., Clay, L., Barral, Y., and Spang, A. (2011) Transport to the plasma membrane is regulated differently early and late in the cell cycle in *Saccharomyces cerevisiae*. *J. Cell Sci.* **124**: 1055-1066.

Zonia, L., and Munnik, T. (2008) Vesicle trafficking dynamics and visualization of zones of exocytosis and endocytosis in tobacco pollen tubes. *J Exp Bot* **59**: 861-873.

## FIGURE LEGENDS

**Figure 1.** Cellular effects of switching from budding growth to mating in *S.cerevisiae*. (A) Chitin was visualized after calcofluor staining. The other images show the localization of the indicated proteins tagged with GFP. (B) Fluorescence after staining with FM4-64. Cells were stained with 10-30 μM FM4-64 at 4ºC. At higher concentrations of FM4-64, fluorescence was distributed along the PM. (C) Localization of actin after staining with Alexa Fluor-488 phalloidin. All images were acquired during vegetative growth (upper row) or after 2 hours in the presence of α-factor (lower row).

**Figure 2.** Microscopic analysis of the assembly of the cellular machinery at the yeast neck. Colocalization of Chs3-GFP, Cdc3-GFP and actin patches with the PM markers Pma1-mCherry and Sur7-mRFP, as indicated in frontal reconstructed (A) or sectional images (B). Note the exclusion zone around the neck for the Pma1 and Sur7 proteins. (C) Colocalization of Chs3-GFP and Cdc3-GFP with the PM marker Pma1-mCherry after LatA treatment. Note the delocalization of Chs3 and the disappearance of the exclusion ring for Pma1 around the neck. (D) Colocalization of Chs3-GFP, Cdc3-GFP and actin patches with the PM marker Pma1-mCherry after PI3K overexpression (see MM for details). (E) Colocalization of Chs3-GFP and Syp1-mCherry. (F) Colocalization of Chs3-GFP with the PM marker Pma1-mCherry in the *syp1*Δ mutant. Note the partial delocalization of Chs3 and the disappearance of the exclusion ring for Pma1 around the neck. All images show living cells, with the exception of cells showing actin patches, which were fixed for Alexa fluor 488-phallodin staining. See also Figure S1 and S2 for additional quantitative data.

**Figure 3.** A model for neck organization. (A) Diameters of the actin patch, Cdc3 and Chs3 rings determined by fluorescence microscopy. The values are means of at least 40 cells and the standard deviations and statistical significance of the differences (#) are indicated. (B) Colocalization of Chs3-GFP and actin patches (Alexa Fluor-568 phallodin). Note the greater diameter of the actin patch ring and its more external positioning. The graph shows fluorescence intensity in both channels along the line labelled in the image. (C) Colocalization of Chs3-GFP and actin patches (Alexa Fluor-568 phallodin) in light microscopy sections. Note the more external positioning of the

actin ring as compared to that of Chs3. (D) A model for the distribution of the different proteins at the neck based on the images presented and on ring diameters (see text for a detailed description).

**Figure 4.** Analysis of Chs3 and Chs4 polarization during mating. Cells containing the indicated plasmids were grown in raffinose medium to early logarithmic phase and then incubated for 2 hours in α-factor. Galactose at 2% was added to the mating medium and protein localization was assessed at the indicated times after induction (galactose addition). Note the initial staining at the tip that later expanded along the mating projections. Note also that Chs3 localization is restricted along the projection while Chs4 eventually diffuses to the cell body. See also Figure S3 for a quantitative analysis of protein distribution.

**Figure 5.** Protein polarization and endocytic turnover during mating. (A) Wt cells after 3 hours of α-factor treatment. Chitin was visualized by calcofluor staining, and Cdc11 by IF. Chs3-GFP localization was assessed in living cells in wt or *chs4*Δ strains. (B) Chs3-GFP does not polarize in the *end4*Δ mutant after α-factor addition. (C) Localization of Chs3-GFP and Snc1-GFP during vegetative growth before and after latA treatment. Note the rapid depolarization of both proteins. (D, E) Effect of latA treatment on the localization of Chs3-GFP and Snc1-GFP during mating. Cells were treated for 25 (D) or 120 (E) minutes with α-factor before the addition of 15 μM latA. Note the polarization of Chs3-GFP and Snc1-GFP, which is maintained after the latA addition for Chs3-GFP but not for Snc1-GFP. Images were acquired before (0) and 35 minutes after the addition of 15μM latA.

**Figure 6.** Analysis of CaChs3-GFP localization in *C.albicans* during yeast or hyphal growth. *C.albicans* cells were grown in YEPD at 28ºC as yeast and then filamentation was induced by the addition of 20% FBS and incubation at 37ºC. (A) localization of CaChs3-GFP at the indicated times after the induction of filamentation. Note the fast polarization of CaChs3-GFP and its accumulation in intracellular structures after 45 minutes in filamentation medium. (B) Localization of CaChs3-GFP in hyphal cells before and after 40 minutes in the presence of 50 μM LatA. Note the tip swelling, but also the maintenance of CaChs3-GFP polarization. (C) Polarization of CaChs3-GFP 40

minutes after the induction of filamentation in the presence of 50 μM LatA. CaChs3 is polarized despite the poor filament formation.

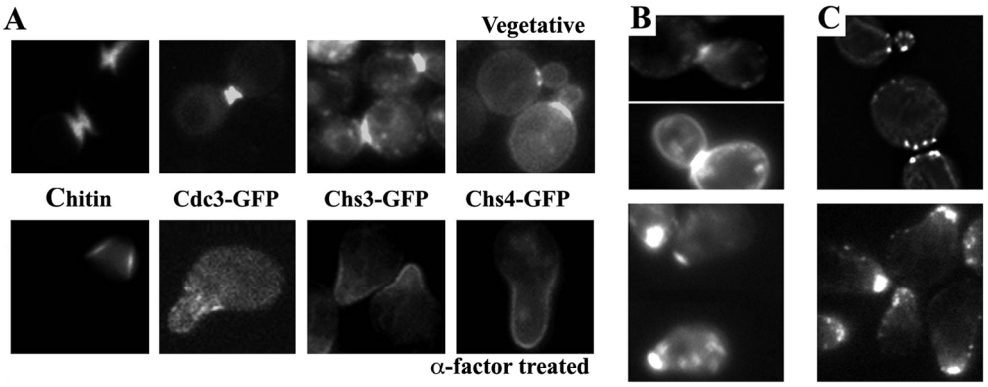


170x69mm (300 x 300 DPI)

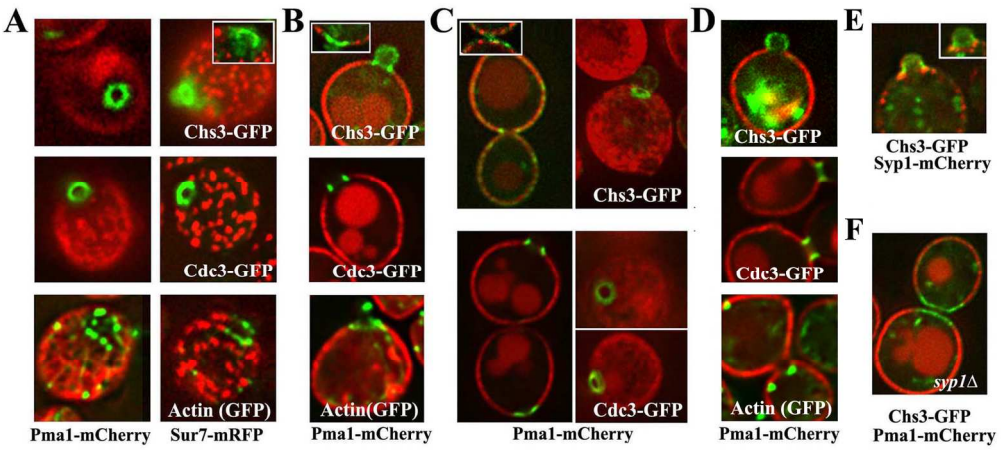


170x76mm (300 x 300 DPI)

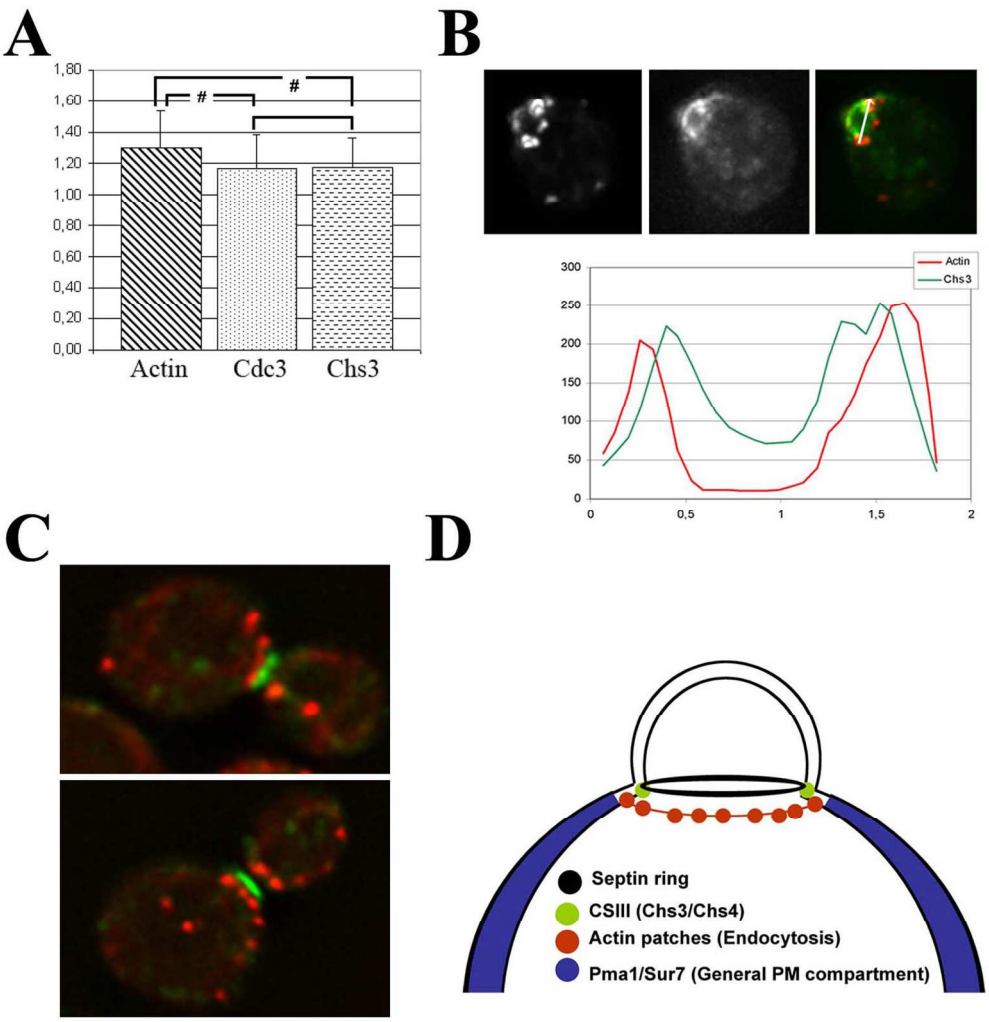


170x174mm (300 x 300 DPI)

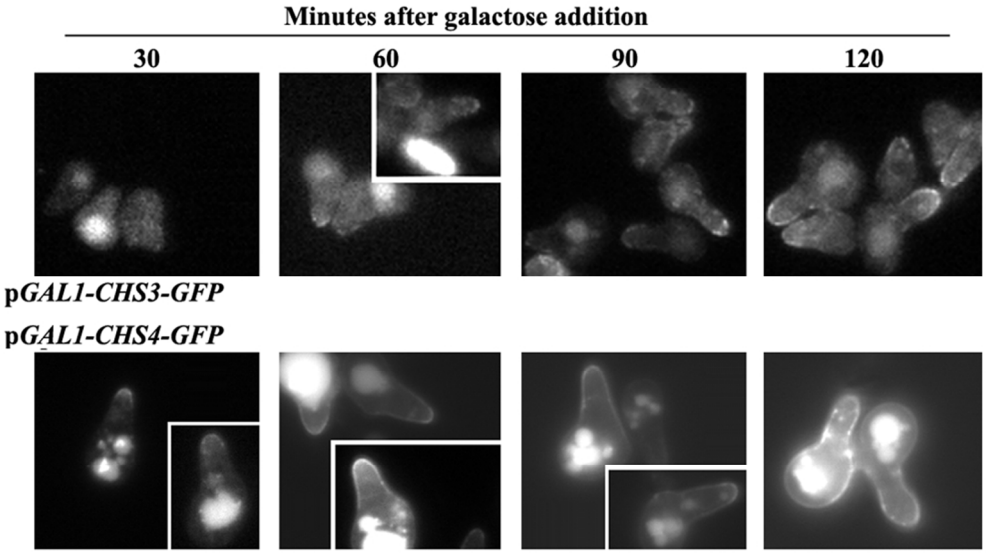


85x47mm (300 x 300 DPI)

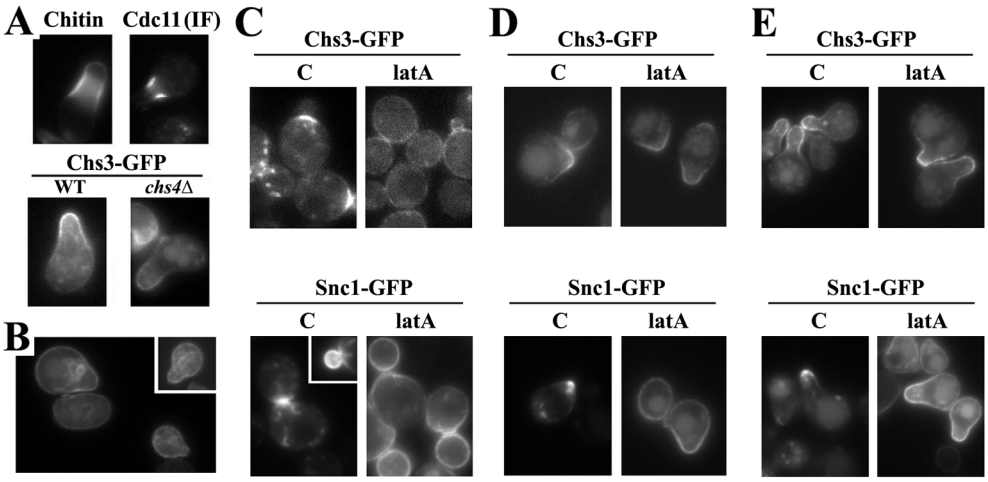


170x84mm (300 x 300 DPI)

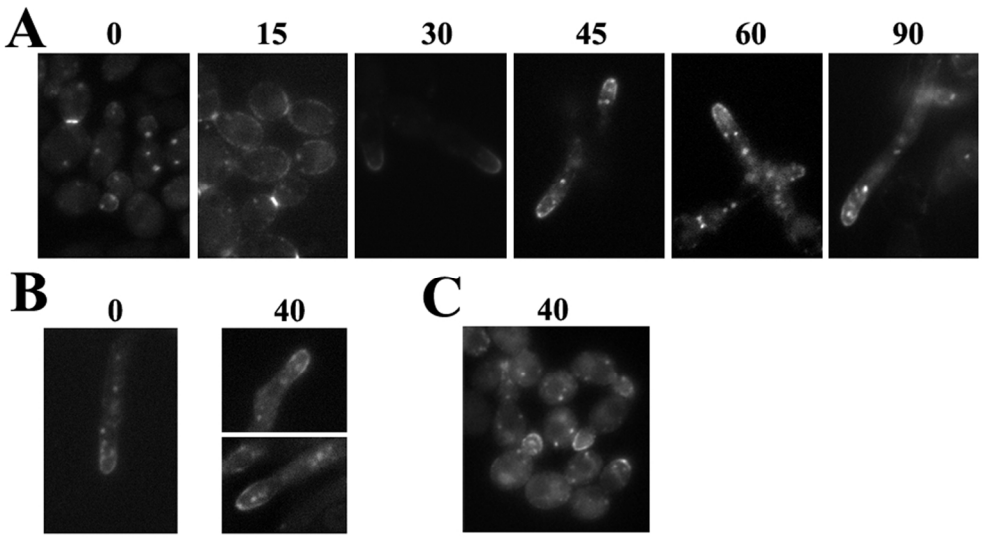


124x70mm (300 x 300 DPI)

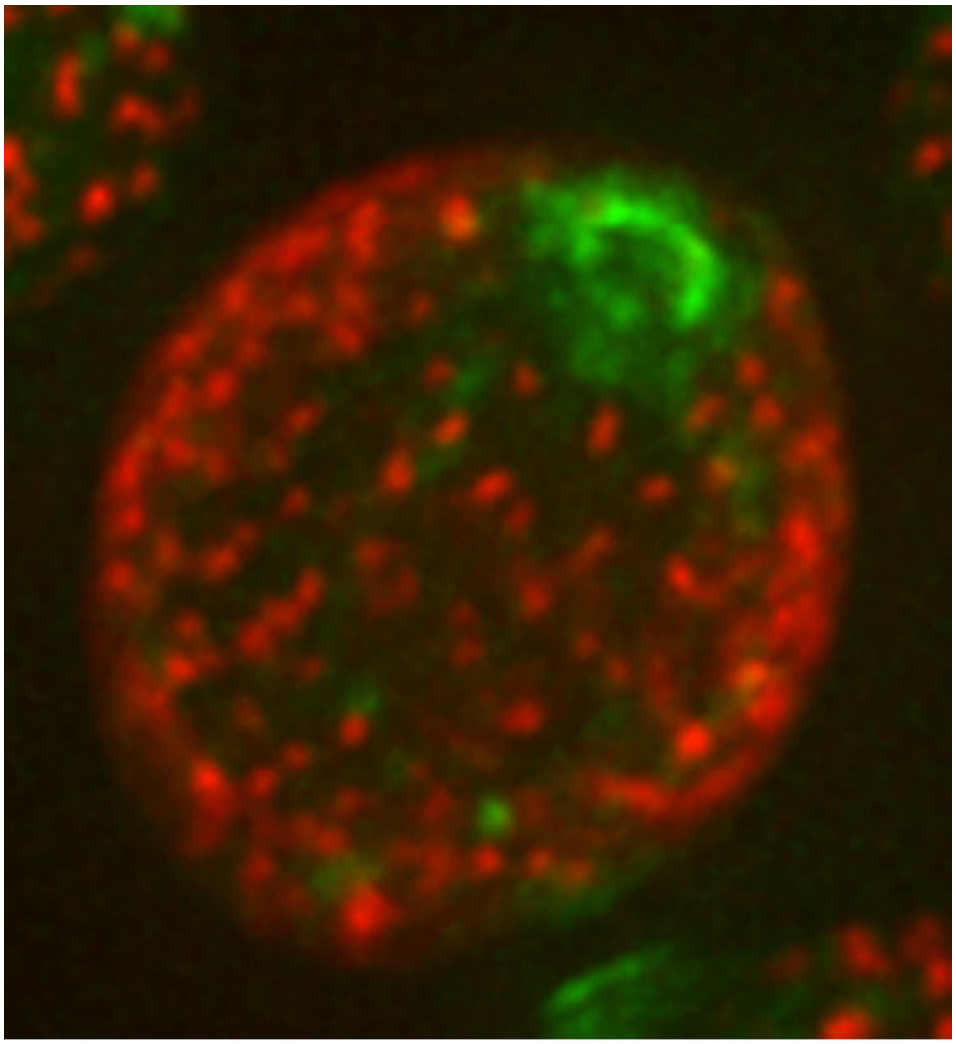

**Neck compartmentalization physically separates different pools of PM proteins: the laterally distributed Sur7-mCherry from the neck protein Chs3-GFP.**

189x240mm (300 x 300 DPI)